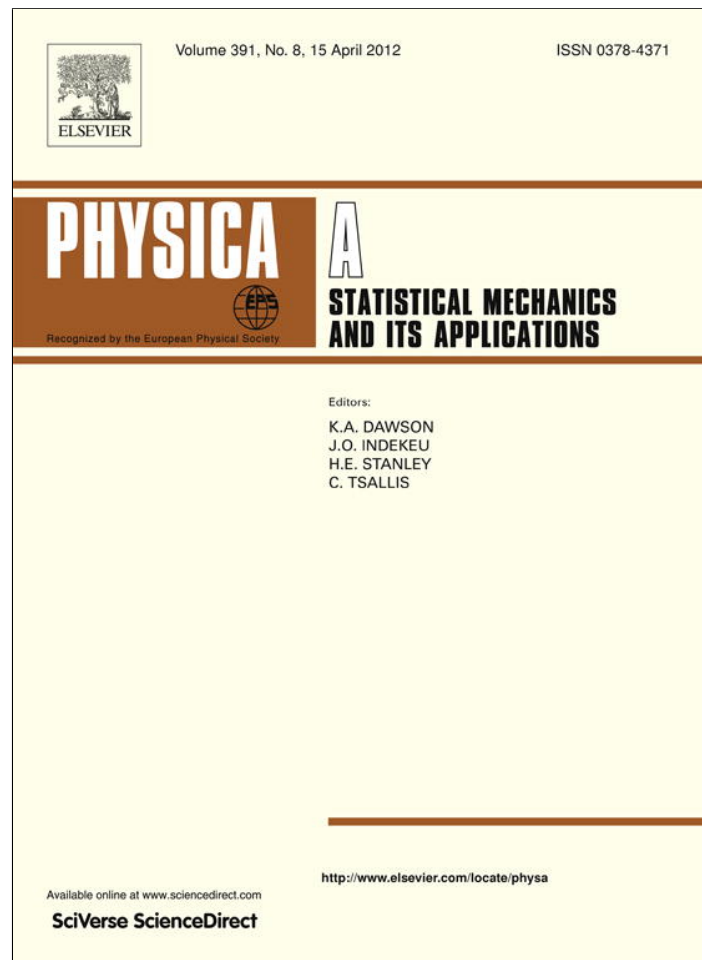


Provided for non-commercial research and education use.
Not for reproduction, distribution or commercial use.



This article appeared in a journal published by Elsevier. The attached copy is furnished to the author for internal non-commercial research and education use, including for instruction at the authors institution and sharing with colleagues.

Other uses, including reproduction and distribution, or selling or licensing copies, or posting to personal, institutional or third party websites are prohibited.

In most cases authors are permitted to post their version of the article (e.g. in Word or Tex form) to their personal website or institutional repository. Authors requiring further information regarding Elsevier's archiving and manuscript policies are encouraged to visit:

<http://www.elsevier.com/copyright>



Contents lists available at SciVerse ScienceDirect

Physica A

journal homepage: www.elsevier.com/locate/physa

Dynamic weight in intelligent transportation systems: A comparison based on two exit scenarios

Chuanfei Dong^{a,*}, Xu Ma^b

^a AOSS Department, College of Engineering, University of Michigan, Ann Arbor, MI 48109, USA

^b Department of Physics, Syracuse University, Syracuse, NY 13244, USA

ARTICLE INFO

Article history:

Received 8 May 2011

Received in revised form 28 November 2011

Available online 13 December 2011

Keywords:

Dynamic weight

Congestion cluster

Exit scenario

Intelligent traffic systems

Cellular automaton model

Velocity distribution

ABSTRACT

Proposing a good exit scenario can make great contributions to improving road conditions. The influence of two exit scenarios, which depend on the dynamic behavior of the last vehicle (that closest to the exit), on the route flux, vehicle number, and speed by using two feedback strategies with different arrival rates (V_p) was studied. We find that the weight of the route is dynamic instead of static, which depends on the real route conditions. In our case study, we find that the flux threshold value with respect to the necessity of applying information feedback strategy is 0.32 (which corresponds to $V_p \approx 0.65$). Further, we illustrate the velocity distribution plots of each route, which provide us with most of the important information we need, when adopting different feedback strategies and exit scenarios with two arrival rates (V_p).

© 2011 Elsevier B.V. All rights reserved.

1. Introduction

In the modern world, traffic congestion problems have become a major issue. Traffic flow and related problems have attracted considerable attention in the past decade [1–5]. Various theories and models have been proposed [6–11] to study the dynamic behavior of vehicular traffic flow, which provide insights that help traffic engineers and other professionals to better manage congestion. Recently, numerous works have been published that report investigations of the dynamic behavior of the traffic flow in scale-free networks [12–19]. Wang and his collaborators [12,13] studied the traffic dynamics based on a local routing protocol in a scale-free network, focusing on both continuous and abrupt phase transitions from a free-flow state to a locally congested state. Besides, they also studied the general dynamics of traffic and routing on a weighted scale-free network [14–16], which is closely related to studies in a weighted traffic system by Dong and his collaborators [20–23]. For example, in the work by Yang et al. [16], they found that there exists an optimal weighting scheme for which cascading failures and traffic congestion can be suppressed significantly; similar results are also shown by Dong et al. [20] in a two-route intelligent traffic system, where they set the weight factor $k = -1.98$ to optimize the road conditions. Further, Barrat, Barthélemy, and Vespignani (BBV) [17] presented an evolutionary model to investigate weighted networks. Inspired by the BBV model, Xie et al. [18] proposed a traffic-driven model to investigate the coevolution of traffic and topology on weighted technological networks by also taking into account the evolution of weight and topology among the old nodes.

Among the large number of research areas, information feedback in intelligent transportation systems (ITSs) has become one of the main streams of research due to its strong capability of improving the road conditions. Recently, some advanced information feedback strategies have been proposed [24–29,22,20,21,23,30,31]. Each feedback strategy has its weakness; for

* Corresponding author. Tel.: +1 4048243966; fax: +1 7346159723.
E-mail address: dcfy@umich.edu (C. Dong).

example, although the Predication Feedback Strategy (PFS) is better than others in terms of improving the road flux [28], the validity of the PFS depends on the length of the route when the transportation system is multi-route, and also the PFS is very time consuming to realize [29]. In order to provide road users with better guidance, a strategy named the Weighted Vehicle Density Feedback Strategy (WVDFS) is presented, which is independent of the length and number of the routes. Further, we investigated the velocity distribution of two routes based on two exit scenarios, depending on the dynamic behavior of the last vehicle, and two different arrival rates V_p , which will be defined in the next section. In the present work, we adopt the two-route model proposed by Wahle et al. [24] with a single route following the Nagel–Schreckenberg mechanism [10] (except for the vehicle closest to the exit).

The structure of the remainder of this paper is as follows. We briefly introduce the NS model, the two-route scenario proposed by Wahle et al. [24], and two feedback strategies, Congestion Coefficient Feedback Strategy [27] and WVDFS, in Section 2. We present and discuss the simulations and analyze the results in Section 3. Finally, we present some conclusions in Section 4.

2. The model and feedback strategies

2.1. NS mechanism and two-route scenario

The rules of the NS mechanism for updating the position x_i of a car are as follows: (i) Acceleration: $v_i(t) \rightarrow v_i(t + \frac{1}{3}) = \min[v_i(t) + 1, v_{\max}]$. (ii) Deceleration: $v_i(t + \frac{1}{3}) \rightarrow v_i(t + \frac{2}{3}) = \min[v_i(t + \frac{1}{3}), g_i(t)]$, so as to avoid collisions, where $g_i(t)$ is the spacing in front of the i th vehicle. (iii) Random brake: with a certain probability p , $v_i(t + \frac{2}{3}) \rightarrow v_i(t + 1) = \max[0, v_i(t + \frac{2}{3}) - 1]$. (iv) Movement: $x_i(t + 1) = x_i(t) + v_i(t + 1)$.

In the NS model, the road is divided into cells (sites) with length $\Delta x = 7.5$ m. The total length of the route is set to be $L = 2000$ cells (corresponding to 15 km). The vehicle density can be defined as $\rho = N/L$, where N denotes the number of vehicles on one route and L is the route length. A time step corresponds to $\Delta t = 1$ s, the typical time a driver needs to react. The flux of one route can be defined as $F = V_{avg}\rho = V_{avg}\frac{N}{L}$, where V_{avg} denotes the average velocity of all the vehicles on one route. In the present paper, we set the maximum velocity $v_{\max} = 3$ cells/time step (corresponding to 81 km/h, and thus a reasonable value) for simplicity.

Recently, Wahle et al. [24] investigated a two-route model. In their model, a percentage of drivers (referred to as dynamic drivers) choose one of the two routes according to the real-time information displayed on the roadside. In their model, the two routes A and B are of the same length L . A new vehicle will be generated at the entrance of the traffic system with arrival rate V_p at each time step. If a driver is a so-called static one, he/she enters a route at random, ignoring any advice. The density of dynamic and static travelers is S_{dyn} and $1 - S_{dyn}$, respectively. Once a vehicle enters one of the two routes, the motion of it will follow the dynamics of the NS model (except the vehicle closest to the exit). In our simulations, a vehicle will be removed after it reaches the end point. It is important to note that, if a vehicle cannot enter the preferred route, it will wait till the next time step rather than entering the unpreferred route.

2.2. Exit scenario

Fig. 1 illustrates the “one entrance and one exit” structure of the traffic system. The first exit scenario is as follows.

- (a) The special velocity update mechanism for the vehicle nearest to the exit is as follows.
 - (i) $velocity(t) = \text{Min}(velocity(t) + 1, 3)$, (probability: 75%).
 - (ii) $velocity(t) = \text{Max}(velocity(t) - 1, 0)$, (probability: 25%).
- (b) The rules at the exit when vehicles are competing for exiting are as follows.
 - (i) At the end of two routes, the vehicle nearer to the exit goes first.
 - (ii) If the vehicles at the end of two routes have the same distance to the exit, the faster a vehicle is driven, the sooner it leaves.
 - (iii) If the vehicles at the end of two routes have the same speed and distance to the exit, the vehicle in the route which has more vehicles leaves first.
 - (iv) If rules (i), (ii), and (iii) are satisfied at the same time, then the vehicles go out randomly.
- (c) $velocity(t) = position(t) - position(t - 1)$, where $position(t) = L = 2000$; (valid only for the vehicles that failed in competing for leaving at the exit).

Here, we want to stress that the vehicle nearest to the exit will not obey the NS mechanism but the special mechanism as shown in rule (a). However, vehicles following the vehicle closest to the exit still obey the NS mechanism. One should also be aware that, if the vehicle nearest to the exit does not compete with the vehicle on the other route for exiting or wins in the competition, the vehicle will ignore rule (c). The special velocity update mechanism (rule (a)) is equivalent to the situation that 75% of drivers exhibit aggressive behavior and 25% of drivers exhibit timid behavior near the exit, which is similar to that in the recent work studied by Laval and Leclercq [32]. However, drivers that exhibit timid behavior at one time step may also exhibit aggressive behavior at another next time step, otherwise timid drivers may stop at the exit forever. Finally, we

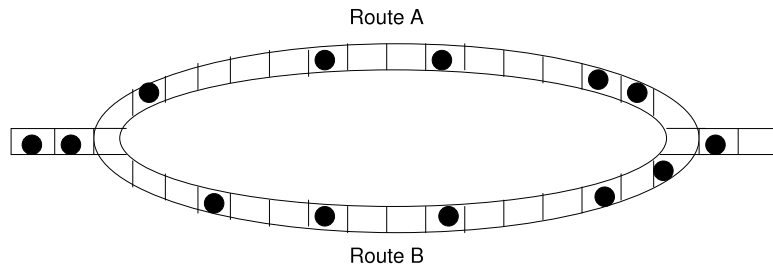


Fig. 1. The one entrance and one exit two-route traffic system.

should clarify that the rules at the exit in Refs. [28,29,20] are the same as those described above, but they were not explained very well in Refs. [20,21,28].

We will also discuss another exit scenario. The difference between the second exit scenario and the first exit scenario is that the vehicle nearest to the exit still obeys the NS mechanism, which means that the vehicle closest to the exit will obey rules (b) and (c) while neglecting rule (a).

2.3. Feedback strategy

CCFS: The position of each vehicle will be known by the signal transmitted from a navigation system (GPS). Then the traffic control center will compute the congestion coefficient of each route based on this information and display it on a board. Road users at the entrance will choose the road with smaller congestion coefficient. The congestion coefficient is defined as [27]

$$C = \sum_{q=1}^m n_q^2. \tag{2.1}$$

Here, n_q stands for the number of vehicles of the q th congestion cluster in which cars are close to each other without a gap between any two of them.

WVDFS: Every time step, the traffic control center will receive data from the navigation system (GPS) like in the CCFS. The work of the traffic control center is to compute the vehicle density of each route with a reasonable weighted function and display it on a board. The road users at the entrance will choose the road with smaller weighted vehicle density. The density of vehicles on each route can be expressed as the number of vehicles N divided by the length L ($\rho = N/L$). Here we use vehicle density instead of number of vehicles because when the lengths of the two routes are different, we should use L to normalize the result.

The WVDFS is based on the Vehicle Density Feedback Strategy (VDFS), where VDFS means that we use the route density without weighted coefficient as the feedback information. Fig. 2 shows the dependence of average flux on arrival rate (V_p) at the entrance of the traffic system by using two feedback strategies with two different exit scenarios. The definition of the arrival rate (V_p) at the entrance is the probability that a vehicle arrives at the entrance at each time step. For example, $V_p = 1$ means that there will be one vehicle arriving at the entrance at each time step and $V_p = 0.4$ means that the probability of vehicles arriving at the entrance at each time step is 0.4. The main conclusion we can draw from Fig. 2 is that the route flux has little relation with feedback strategies and exit scenarios when $V_p \leq 0.65$. The slope of the curves adopting different feedback strategies and exit scenarios is almost constant when $V_p \leq 0.65$, indicating that vehicles can always enter the route immediately after they arrive the entrance until V_p increases to 0.65. With persistent increase of V_p , the feedback strategy and exit scenario will greatly affect the route flux. The decrease of the route flux is primarily caused by the fact that vehicles cannot enter the route immediately after they arrive the entrance when V_p increases to some point. Given that V_p varies according to time of day, we think that the VDFS is better than the CCFS no matter which exit scenario adopted. In this study, we investigated two cases: $V_p = 0.6$ and $V_p = 1.0$.

The weighted vehicle density is defined as

$$\rho_w = \sum_{i=1}^N \frac{F(n_i)}{L}. \tag{2.2}$$

Here, n_i stands for the position of the i th vehicle and N stands for the total number of vehicles on the route at that moment. $F(x)$ is the weighted function of each route.

After we tried some functions such as $F(x) = \sin(ax + b) + c$, the exponential function, and the Gaussian function, we found that $F(x) = kx + b$ is the optimal one in terms of improving the capacity of the road. In this study, we set $b \neq 0$ because it will cause the absolute weight value of the first route site always to be the smallest when $b = 0$. In the present work, we assume that $b = 2.0$. We also tried functions such as $F(x) = kx^n + b$ ($n > 1$) and found that the power exponent n makes almost no contributions to the results. Thus we obtained the following function:

$$F(x) = k \times x + b = k \times \frac{n_i}{2000} + 2.0. \tag{2.3}$$

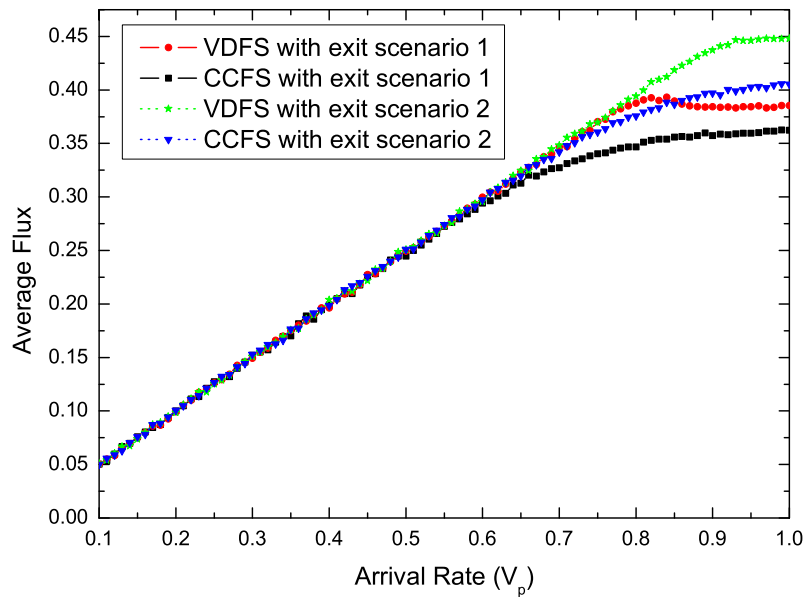


Fig. 2. (Color online) Average flux versus arrival rate (V_p) at the entrance of the transportation system. The parameters are $L = 2000$, $p = 0.25$, and $S_{dyn} = 1.0$.

Finally, the expression for ρ_w becomes

$$\rho_w = \sum_{i=1}^N \frac{F(n_i)}{L} = \sum_{i=1}^N \frac{(k \times \frac{n_i}{2000} + 2.0)}{L}. \quad (2.4)$$

We found that the weight factor (slope – k) will directly affect the road capacity, which will be discussed explicitly in Section 3.

Finally, we point out that we initially set the routes and boards empty and let vehicles enter the routes randomly during the initial 100 time steps in the simulation. Thus, the feedback starting at the 101st second is based on the 100th second route state. In simulations, vehicles can enter the preferred route only when the first three sites of the route are empty in order to avoid collisions. In the following section, the performance of two different feedback strategies will be shown and discussed in detail.

3. Simulation results and discussions

Fig. 3 shows the dependence of average flux on weight factor (k) by adopting the WVDFS with two different exit scenarios and arrival rate V_p . Fig. 3 is based on an average of ten simulations. Here, the physical sense of flux F is the number of vehicles passing the exit of the traffic system each time step. Therefore the larger the value of F , the better processing capacity the traffic system has. As to the routes' processing capacity, the highest positive peak structure is located in the vicinity of $k \sim 2.9$ (refer to Fig. 3(a)). Thus, the value of k_1 is fixed at 2.9 when adopting the first exit scenario with $V_p = 1.0$. One may be puzzled why, when adopting the WCCFS, the positive peak structure is located in the vicinity of $k \sim -1.98$ [20]. Actually, this is one of the issues, namely *dynamic weight*, that we want to discuss in this paper. In Fig. 3(b), there is no obvious peak structure, whereas the flux values in the range $-3.0 < k_2 < -1.0$ are higher than in the surroundings. So we set $k_2 = -2.0$ when adopting the second exit scenario with $V_p = 1.0$, which is very similar to the value in Ref. [20]. From the results shown in Fig. 3(a) and (b), we know that the weight of the route depends on the real route conditions. In other words, the weight of the system is dynamic instead of static, which may give us some clues to the origins of the different weight value discussed above. The weight value of the entrance is much smaller than that of the exit when adopting the WVDFS with the first exit scenario under $V_p = 1.0$, which means that the exit of the traffic system is more important than the entrance under these conditions. Conversely, when adopting the second exit scenario, the weight of the entrance is larger than that of the exit. The reason can be explained as follows.

When adopting the first exit scenario, there is a high possibility to form a jammed state at the end of the route due to both the deceleration of vehicles nearest to the exit and the one-exit structure of the traffic system. Therefore, the exit is more important than the entrance. In this situation, the rate of vehicles entering the system is larger than the rate of vehicles leaving the system at the beginning, and the system will be saturated in a period of time, which is also indicated by Fig. 2 (referring to the changing of the slope). Here, the route-saturated state means that the average speed of the route reaches the lower limit or the number of vehicles the route can accommodate reaches the upper limit. This result is closely related to the studies by Wang et al. [12,13], where they studied the phase transition from a free-flow state to a locally congested state. The saturated state of the route actually is the same as the congestion state described in Refs. [12,13]. Analogously,

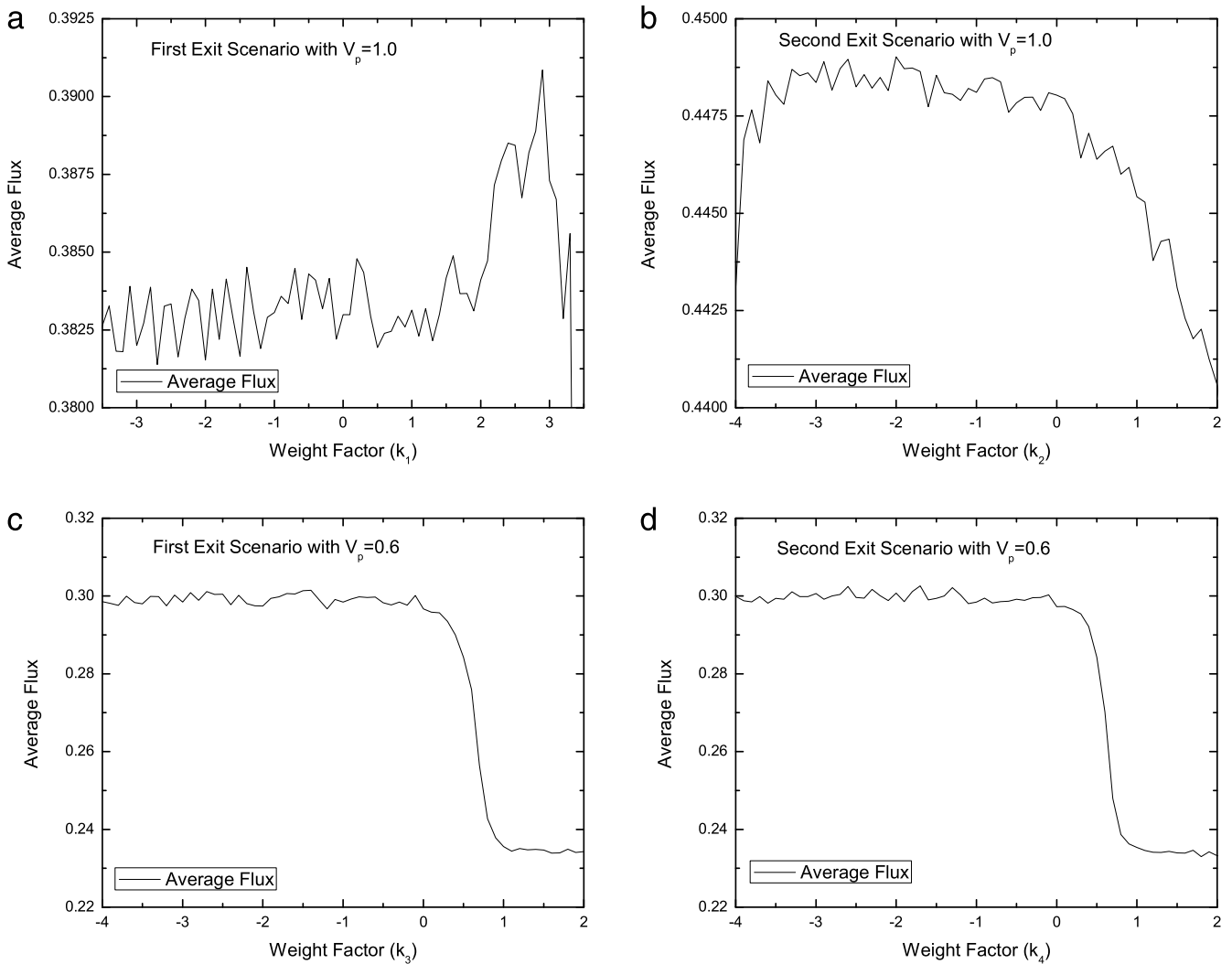


Fig. 3. (a) Average flux versus weight factor (k_1) with first exit scenario ($V_p = 1.0$). (b) Average flux versus weight factor (k_2) with second exit scenario ($V_p = 1.0$). (c) Average flux versus weight factor (k_3) with first exit scenario ($V_p = 0.6$). (d) Average flux versus weight factor (k_4) with second exit scenario ($V_p = 0.6$). The parameters are $L = 2000$, $p = 0.25$, and $S_{dyn} = 1.0$.

the unsaturated state of the traffic system is the free-flow state. While adopting the second exit scenario, the rate of vehicles leaving the system is larger than that adopting the first exit scenario. Under these circumstances, the possibility of jammed states occurring at the end of the route becomes lower, and thus the entrance becomes more important than the exit.

Fig. 3(c) and (d) show almost the same tendency, which indicates that the different exit scenarios make little contribution to the route conditions when V_p is relatively low. In this situation, the rate of vehicles entering the system is approximately equal to the rate of vehicles leaving the system; therefore the system is unsaturated. It is impossible for a traffic jam to occur at the end of the route. Hence, the entrance becomes more important than the exit when V_p is relatively low, no matter which exit scenario is adopted.

In Fig. 4, we illustrate the unnormalized velocity distribution of each route when adopting the CCFS and the WVDFS with two exit scenarios and two different arrival rates (V_p). The results of Fig. 4 are based on the average of 5000 time steps (15000th–20000th time step). From Fig. 4(a), (b), (e), and (f), we know that, even though the same feedback strategy is applied, the dynamic behavior of the last vehicle will greatly affect the velocity distribution of all the vehicles on this route when $V_p = 1$, which is also indicated by Refs. [4,33]. Compared with the second exit scenario, the first exit scenario results in a great number of vehicles with low speed and even zero velocity, especially for the case of the WVDFS (refer to Fig. 4(e)). This is caused by the jammed state at the end of the route when adopting the first exit scenario. Fig. 4(e) and (f) can also explain the reason why the weights are so different when adopting the WVDFS with the first and second exit scenarios. The low speed shown in Fig. 4(e) indicates there should be traffic congestion at the end of the route. The larger exit weight can make the vehicle density at the end of the route larger than it should be. This is equivalent to the fact that the feedback strategy amplifies the negative effects caused by the traffic jams at the end of the route, which will cause any vehicle at the entrance to tend to wait instead of entering the route. Thus, the feedback can prevent the jammed state from further exacerbation. On the other hand, the speed adopting the

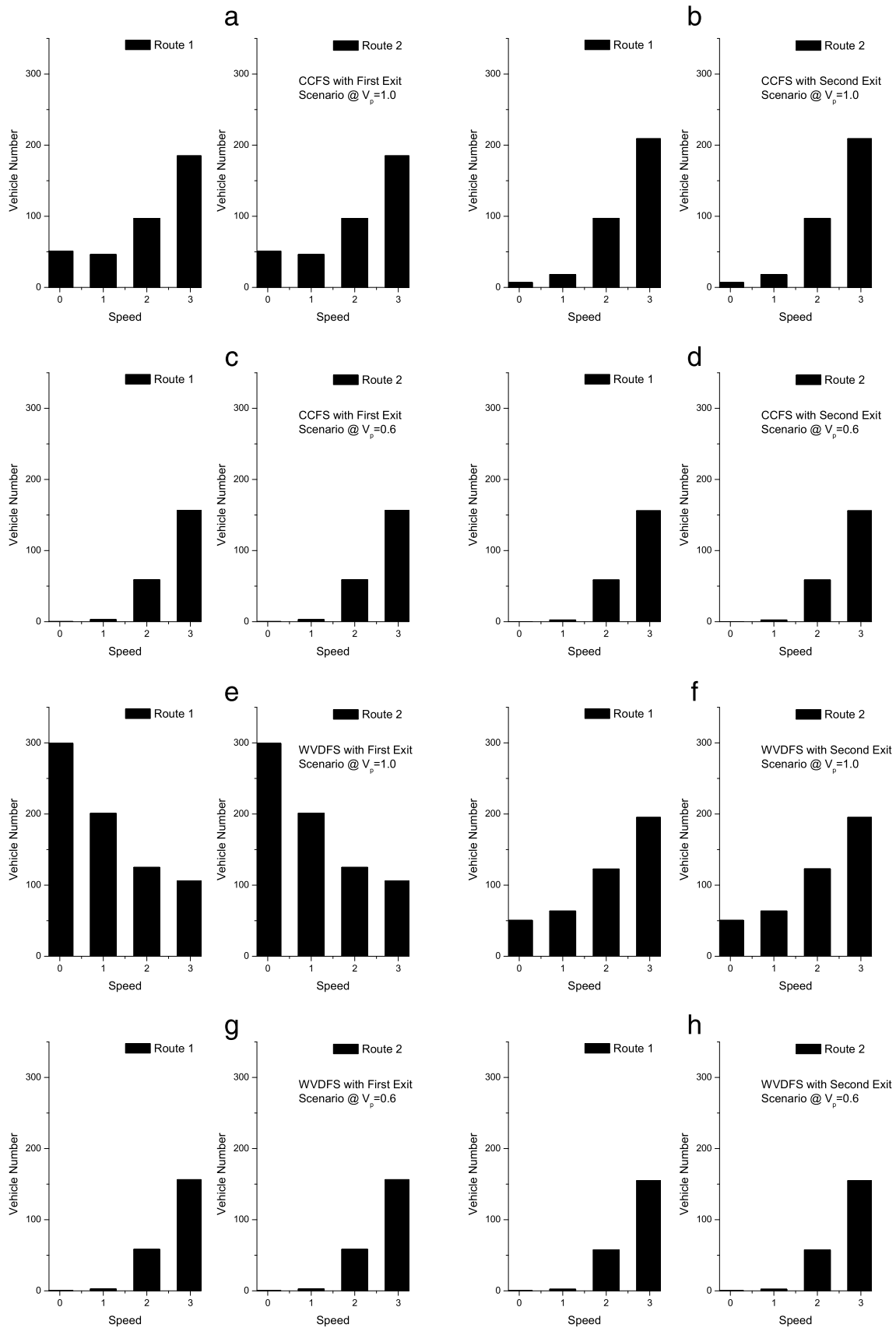


Fig. 4. Velocity distribution of each route with different exit scenarios and arrival rates (V_p): CCFS (first row), and WVDFS (second row). The parameters are $L = 2000$, $p = 0.25$, $S_{dyn} = 0.5$, and weight factors $k_1 = 2.9$, $k_2 = -2.0$, $k_3 = -2.0$, and $k_4 = -2.0$.

Table 1
The corresponding values of Fig. 4.

Figure number		F_{avg}	N	v_{avg}
Fig. 4(a)	CCFS with first exit scenario when $V_p = 1.0$	0.381	399	1.91
Fig. 4(b)	CCFS with second exit scenario when $V_p = 1.0$	0.424	342	2.48
Fig. 4(c)	CCFS with first exit scenario when $V_p = 0.6$	0.290	215	2.70
Fig. 4(d)	CCFS with second exit scenario when $V_p = 0.6$	0.292	215	2.71
Fig. 4(e)	WVDFS with first exit scenario when $V_p = 1.0$	0.382	747	1.02
Fig. 4(f)	WVDFS with second exit scenario when $V_p = 1.0$	0.448	440	2.04
Fig. 4(g)	WVDFS with first exit scenario when $V_p = 0.6$	0.295	219	2.69
Fig. 4(h)	WVDFS with second exit scenario when $V_p = 0.6$	0.295	220	2.68

WVDFS with the second exit scenario (refer to Fig. 4(f)) is much larger than that of the first exit scenario, indicating that the possibility of traffic jams occurring at the end of the route is much smaller. In this situation, entering the route with better conditions plays a more important role in the traffic system, so the entrance weight is larger than the exit weight.

However, when the arrival rate is relatively low, i.e., $V_p = 0.6$, the velocity distributions show almost the same tendency no matter what feedback strategies and exit scenarios are adopted (see Fig. 4(c), (d), (g), and (h)). This indicates that the traffic system is unsaturated when V_p is lower than some value. In this situation, the feedback strategy and exit scenario make little impact on the road conditions. From Fig. 1, we know that this threshold value is around 0.65, and the corresponding average flux is approximately equal to 0.32. This is similar to the results shown by Wang et al. [12,13] in a scale-free traffic network, in which there is a critical point that controls the phase transition from free flow to congestion. Thus the route adopting the WVDFS with the first exit scenario under $V_p = 1.0$ is saturated due to the high number of vehicles, and it reaches the upper limit (~ 750). The macroscopic merging behavior of traffic at fully congested freeway merges has been investigated by Bar-Gera and Ahn [33] as well by the archived traffic data in the California PEMS (Performance Measurement System) from January 2004 to June 2008. Our simulation results shown above are also consistent with the empirical study of phase transition by Mukherjee and Manna [19] and empirical observation of a phase transition from a free-flow state to a congested state by Takayasu et al. [34].

Here, we want to stress that the unnormalized velocity distribution plot is very useful; it has never been shown before in a weighted traffic network. From this plot, we can obtain a lot of information, i.e., the total vehicle number on each route ($N = \sum_{i=0}^3 N_i$), the average velocity of each route ($v_{avg} = \sum_{i=0}^3 v_i \times N_i / N$), and the average flux of each route ($F_{avg} = N / L \times v_{avg}$). Table 1 shows the corresponding values of Fig. 4. It demonstrates again that when $V_p = 0.6$ the results adopting different feedback strategies and exit scenarios are almost the same, while, when $V_p = 1.0$, the feedback strategy and exit scenario will greatly affect the results. The high flux of the WVDFS adopting the first scenario is mainly contributed by the high number of vehicles.

Fig. 5 shows the relation between average flux and density of dynamic travelers (S_{dyn}) by using two different feedback strategies with two exit scenarios. The dynamic behavior of the last vehicle can great affect the route flux, as indicated by Fig. 4. As to the routes' processing capacity, the new strategy with the second exit scenario is the best one (refer to Fig. 5(b)). One interesting thing here is that, when $V_p = 0.6$, the fluxes adopting different feedback strategies and exit scenarios show almost the same tendency with the increase of S_{dyn} , indicating that there is no need to use feedback in a traffic system when the local vehicle flux is relatively low. However, when $V_p = 1.0$, different feedback strategies and exit scenarios will greatly affect the route capacity. The practicability of a feedback strategy depends on the fact that the capacity of the route adopting this strategy ($S_{dyn} = 1$) is better than that in the situation of vehicles entering the route randomly ($S_{dyn} = 0$). Hence, the WVDFS is an optimal information feedback strategy.

The optimal information feedback strategies proposed in this paper can be realized by adopting the data provided by some experimental or empirical measurements, such as using TerraSAR-X Along-Track Interferometry [35], and the automatic measurement of traffic variables proposed by Nam and Drew [36].

4. Conclusion

In summary, we investigated the change of road conditions with weight factor (k), arrival rate (V_p), and dynamic driver density (S_{dyn}). We also studied the velocity distribution of each route in different situations, which can provide us with the essential information we need. The route weight depends on the real route conditions, which in turn demonstrates that the weight of the route is not static but dynamic. When the route is saturated, the route exit usually has a larger weight value than the entrance; otherwise, the entrance is more important than the exit.

Besides, we find that, when the flux is relatively low, there is no obvious difference between the route conditions by adopting different feedback strategies (including the random case ($S_{dyn} = 0$)) and exit scenarios. However, when the flux becomes sufficiently large, the feedback strategies and exit scenarios will greatly affect the route conditions, indicating that it is essential to apply an optimal information feedback strategy with a good exit scenario to intrinsically improve the route capacity. As shown by the simulations, adopting the WVDFS with the second exit scenario is the optimal one among all the cases studied in a "one entrance and one exit" traffic system. In our case study, we find that the threshold value in the

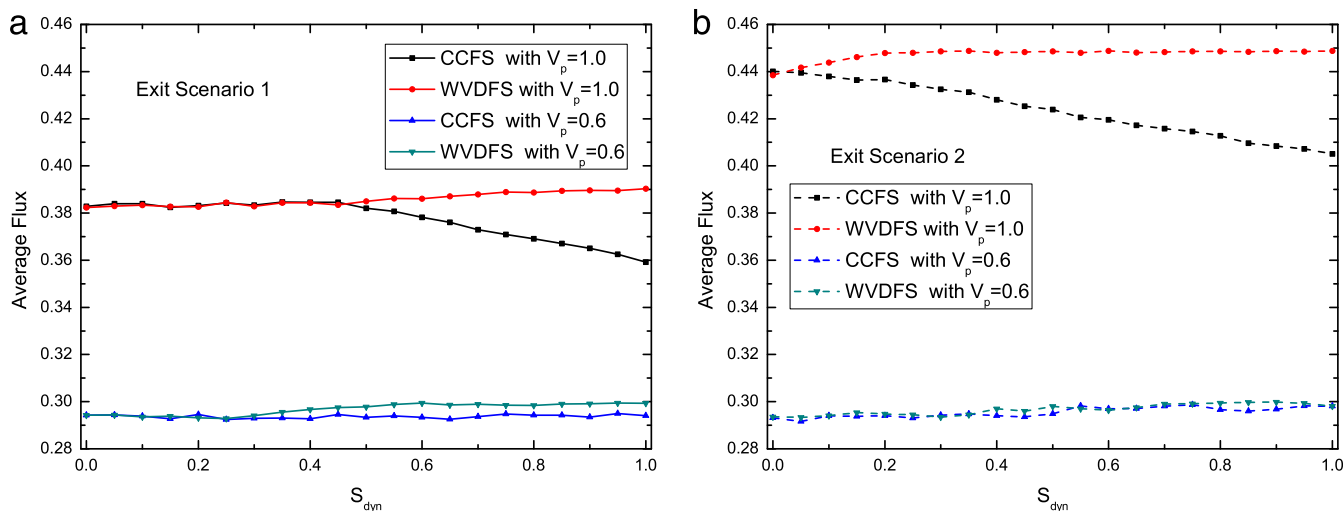


Fig. 5. (Color online) Average flux by performing different strategies and exit scenarios versus S_{dyn} ; L is fixed at 2000, p is fixed at 0.25, and the weight factors $k_1 = 2.9$, $k_2 = -2.0$, $k_3 = -2.0$, and $k_4 = -2.0$.

present work is around 0.32; similar results are also obtained by Wang et al. [12,13] in a scale-free network, where they found that the network capacity can be measured by the critical point of the phase transition from free flow to congestion. An advanced information feedback strategy can make great contributions to improving the road capacity only when the flux becomes relatively high. Therefore, for large modern cities, applying an optimal feedback strategy in a real-time traffic system is appropriate and indispensable. Taking into account the reasonable cost and more accurate description of road condition, we think that the new feedback strategy will make great contributions to radically improve the road conditions of high-flux real-time traffic systems.

Acknowledgments

C.F. Dong would like to thank Dr. N. Liu at the University of Chicago for some helpful comments while preparing the manuscript.

References

- [1] D. Chowdhury, L. Santen, A. Schadschneider, Phys. Rep. 329 (2000) 199.
- [2] D. Helbing, Rev. Modern Phys. 73 (2001) 1067.
- [3] T. Nagatani, Rep. Progr. Phys. 65 (2002) 1331.
- [4] G. Orosz, R.E. Wilson, G. Stépán, PTRSA 368 (2010) 4455.
- [5] B.K. Chen, Y.B. Xie, W. Tong, C.F. Dong, D.M. Shi, B.H. Wang, A comprehensive study of advanced information feedbacks in real-time intelligent traffic systems, Physica A (2011), doi:10.1016/j.physa.2011.12.032.
- [6] R.W. Rothery, Traffic flow theory, in: N. Gartner, C.J. Messner, A.J. Rathi (Eds.), in: Transportation Research Board Special Report, vol. 165, Transportation Research Board, Washington, D.C., 1992 (Chapter 4).
- [7] S.L. Paveri-Fontana, Transp. Res. 9 (1975) 225.
- [8] C. Wagner, C. Hoffmann, R. Sollacher, J. Wagenhuber, B. Schürmann, Phys. Rev. E 54 (1996) 5073.
- [9] D. Helbing, M. Treiber, Phys. Rev. Lett. 81 (1998) 3042.
- [10] K. Nagel, M. Schreckenberg, J. Phys. 12 (1992) 2221.
- [11] O. Biham, A.A. Middleton, D. Levine, Phys. Rev. A 46 (1992) R6124.
- [12] W.X. Wang, B.H. Wang, C.Y. Yin, Y.B. Xie, T. Zhou, Phys. Rev. E 73 (2006) 026111.
- [13] W.X. Wang, Z.X. Wu, R. Jiang, G.R. Chen, Y.C. Lai, Chaos 19 (2009) 033106.
- [14] W.X. Wang, B.H. Wang, B. Hu, G. Yan, Q. Ou, Phys. Rev. Lett. 94 (2005) 188702.
- [15] M.B. Hu, R. Jiang, W.X. Wang, Q.S. Wu, Y.H. Wu, Physica A 387 (2008) 4967.
- [16] R. Yang, W.X. Wang, Y.C. Lai, G.R. Chen, Phys. Rev. E 79 (2009) 026112.
- [17] A. Barrat, M. Barthélemy, A. Vespignani, Phys. Rev. Lett. 92 (2004) 228701; Phys. Rev. E 70 (2004) 066149.
- [18] Y.B. Xie, W.X. Wang, B.H. Wang, Phys. Rev. E 75 (2007) 026111.
- [19] G. Mukherjee, S.S. Manna, Phys. Rev. E 71 (2005) 066108.
- [20] C.F. Dong, X. Ma, B.H. Wang, Phys. Lett. A 374 (2010) 1326.
- [21] C.F. Dong, X. Ma, Phys. Lett. A 374 (2010) 2417.
- [22] C.F. Dong, C.S. Paty, Inform. Sci. 181 (2011) 5042.
- [23] B.K. Chen, X.Y. Sun, H. Wei, C.F. Dong, B.H. Wang, Internat. J. Modern Phys. C 22 (2011) 849.
- [24] J. Wahle, A.L.C. Bazzan, F. Klügl, M. Schreckenberg, Physica A 287 (2000) 669.
- [25] J. Wahle, A.L.C. Bazzan, F. Klügl, M. Schreckenberg, Transp. Res., Part C 10 (2002) 399.
- [26] K. Lee, P.M. Hui, B.H. Wang, N.F. Johnson, J. Phys. Soc. Japan 70 (2001) 3507.
- [27] W.X. Wang, B.H. Wang, W.C. Zheng, C.Y. Yin, T. Zhou, Phys. Rev. E 72 (2005) 066702.
- [28] C.F. Dong, X. Ma, G.W. Wang, X.Y. Sun, B.H. Wang, Physica A 388 (2009) 4651.
- [29] C.F. Dong, X. Ma, B.H. Wang, X.Y. Sun, Physica A 389 (2010) 3274.
- [30] C.F. Dong, X. Ma, B.H. Wang, Internat. J. Modern Phys. C 21 (2010) 1081.
- [31] C.F. Dong, X. Ma, B.H. Wang, Sci. China Inf. Sci. 53 (2010) 2265.
- [32] J.A. Laval, L. Leclercq, PTRSA 368 (2010) 4519.
- [33] H. Bar-Gera, S. Ahn, Transp. Res., Part C 18 (2010) 457.
- [34] M. Takayasu, H. Takayasu, T. Sato, Physica A 233 (1996) 824.
- [35] S. Suchandt, H. Runge, H. Breit, U. Steinbrecher, A. Kotenkov, U. Balss, IEEE Trans. Geosci. Remote Sens. 48 (2010) 807.
- [36] D.H. Nam, D.R. Drew, Transp. Res., Part B 33 (1999) 437.